

Synthetic shRNAs as potent RNAi triggers

Despina Siolas^{1,2}, Cara Lerner³, Julja Burchard³, Wei Ge³, Peter S Linsley³, Patrick J Paddison², Gregory J Hannon² & Michele A Cleary³

Designing potent silencing triggers is key to the successful application of RNA interference (RNAi) in mammals. Recent studies suggest that the assembly of RNAi effector complexes is coupled to Dicer cleavage. Here we examine whether transfection of optimized Dicer substrates results in an improved RNAi response. Dicer cleavage of chemically synthesized short hairpin RNAs (shRNAs) with 29-base-pair stems and 2-nucleotide 3' overhangs produced predictable homogeneous small RNAs comprising the 22 bases at the 3' end of the stem. Consequently, direct comparisons of synthetic small interfering RNAs and shRNAs that yield the same small RNA became possible. We found synthetic 29-mer shRNAs to be more potent inducers of RNAi than small interfering RNAs. Maximal inhibition of target genes was achieved at lower concentrations and silencing at 24 h was often greater. These studies provide the basis for an improved approach to triggering experimental silencing via the RNAi pathway.

Many eukaryotic organisms respond to double-stranded RNA (dsRNA) by activating a sequence-specific silencing pathway RNAi. RNAi is initiated when an RNase III-family nuclease, Dicer, processes dsRNAs into ~22-nucleotide (nt) fragments known as small interfering (siRNAs)¹⁻³. These small RNAs are used as guides for selection and cleavage of complementary mRNAs through their incorporation into the RNAi effector complex (RISC)^{1,2,4}, whose catalytic subunit, Argonaute 2, has recently been identified^{5,6}. These mechanistic insights have led to approaches for experimentally programming the RNAi machinery in mammalian cells by directly transfecting chemically synthesized siRNA duplexes of ~21 nt, consisting of 19 paired bases with 2-nt 3' overhangs, to produce a transient silencing response⁷.

In many organisms, the RNAi machinery also serves as an effector for endogenous, noncoding RNAs known as microRNAs (miRNAs)⁸. miRNAs are initially generated as long primary transcripts (pri-miRNA) which are cleaved in the nucleus by another RNase III-family nuclease, Drosha⁹. The liberated pre-miRNAs are exported to the cytoplasm, where Dicer performs a second cleavage to produce small RNAs that are loaded into RISC¹⁰⁻¹². In the case of miRNAs, the cleavage sites are specific, and most often a single, discrete sequence is liberated from the precursor⁸. These discoveries prompted the development of a second approach for triggering RNAi in mammalian

cells using DNA vectors encoding shRNAs, modeled roughly after endogenous microRNAs¹³⁻¹⁵.

Remarkably, for both miRNAs and siRNAs, the two strands of the processed dsRNA are treated unequally. In a variety of organisms, cloning has overwhelmingly yielded one strand for each miRNA⁸. A potential explanation for this outcome came from biochemical studies of siRNAs in *Drosophila melanogaster* that suggested that relative thermodynamic instability at the 5' end of a strand of a Dicer product favors its loading into RISC¹⁶. This is in accord with analysis of predicted Dicer cleavage products of endogenous miRNAs¹⁷ and studies of the efficacy of large numbers of siRNAs, which indicate that greater suppression occurs if the antisense strand (relative to the target mRNA) has an unstable 5' end¹⁷. Recent reports have suggested that this loading might occur in a complex and might be coordinated with Dicer cleavage¹⁸⁻²⁰. These mechanistic insights suggest that Dicer substrates might be more efficiently incorporated into RISC than siRNAs. To compare the efficiency of silencing triggers predicted to produce equivalent RISC enzymes, we sought to understand how Dicer processes shRNAs.

We began by producing ~70 chemically synthesized shRNAs, targeting various endogenous genes and reporters. We focused on a detailed analysis of one set of four shRNAs that target firefly luciferase (**Fig. 1a**). The individual species differed in two ways. First, the stems of the shRNAs were either 19 or 29 base pairs (bp) long; these sizes reflect the two stem sizes most commonly used for vector-expressed shRNAs. Second, each shRNA either did or did not contain a 2-nt 3' overhang, identical to that produced by the processing of pri-miRNAs by Drosha. Each species was end labeled by enzymatic phosphorylation and incubated with recombinant human Dicer. The 29-mer shRNA with the 3' overhang was converted almost quantitatively into a 22-nt product by Dicer (**Fig. 1b**). In contrast, the 29-mer shRNA without the overhang generated very little discrete 22-nt labeled product, despite a Dicer-dependent depletion of the starting material. Neither 19-mer shRNA was cleaved to a detectable level by the Dicer enzyme. This result was not due to the lack of double-stranded structure in the 19-mer shRNAs, as all shRNA substrates were efficiently cleaved by bacterial RNase III (**Supplementary Fig. 1** online). Rather, these results suggest that the shRNAs with a 3' overhang produced predominantly one specific and unique small RNA product, whereas a blunt-ended hairpin was processed into a range of products. This hypothesis was consistent with parallel analysis

¹Program in Genetics, Stony Brook University, Stony Brook, New York 11794, USA. ²Cold Spring Harbor Laboratory, Watson School of Biological Sciences, 1 Bungtown Road, Cold Spring Harbor, New York 11724, USA. ³Rosetta Inpharmatics, LLC, a wholly owned subsidiary of Merck and Co., Inc., 401 Terry North, Seattle, Washington 98109, USA. Correspondence should be addressed to G.J.H. (hannon@cshl.edu) and M.A.C. (michele_cleary@merck.com).

of identical shRNA substrates that were produced by *in vitro* transcription with T7 polymerase and uniformly labeled (Fig. 1c). Uniformly labeled 29-mer shRNAs both with and without overhangs produced cleavage products, with the latter being less abundant. Additionally, shRNAs with overhangs yielded products of two discrete sizes (21 and 22 nt). Considered together, our results suggest that Dicer requires a minimum stem length for efficient cleavage. Furthermore, they are consistent with the hypothesis that the presence of a correct 3' overhang enhances the efficiency and specificity of cleavage, directing Dicer to cut ~22 nt from the end of the substrate.

A number of previous studies have suggested that Dicer might function as an end-recognizing endonuclease without positing a role for the 3' overhang. Blocking the ends of dsRNAs using either fold-back structures or chimeric RNA-DNA hybrids attenuated, but did not abolish, the ability of human Dicer to generate siRNAs²¹. One group suggested that Dicer cleaved ~22 nt from the blunt end of an extended pre-miRNA, designed in part to mimic a pri-miRNA²². Structural analysis of the Argonaute 2 PAZ domain suggested that it engages very short (~2- to 3-nt) stretches of the 3' ends of single-stranded RNAs^{23–26}. This led another group of researchers to propose a model in which the 3' overhangs of pre-miRNAs, generated by Drosha cleavage, serve as an important recognition and specificity determinant for subsequent processing by Dicer²⁵. The results presented here are consistent with this model and suggest further that the 3' overhang aids in determining the specificity of cleavage, directing processing to a site 22 nt from the 3' end of the substrate. These findings are in full accord with a recently published model for Dicer action²⁷.

To validate our biochemical analysis, we also mapped the position of Dicer cleavage *in vivo* using primer extension. Precursors were transfected into cells, and the processed form of each was isolated by coimmunoprecipitation with the coexpressed Myc-tagged human Argonaute proteins Ago1 and Ago2. The 29-mer shRNA with an overhang gave rise to a relatively discrete product of 20 nt as predicted for a cleavage 22 nt from the 3' end of the substrate. Primer extension

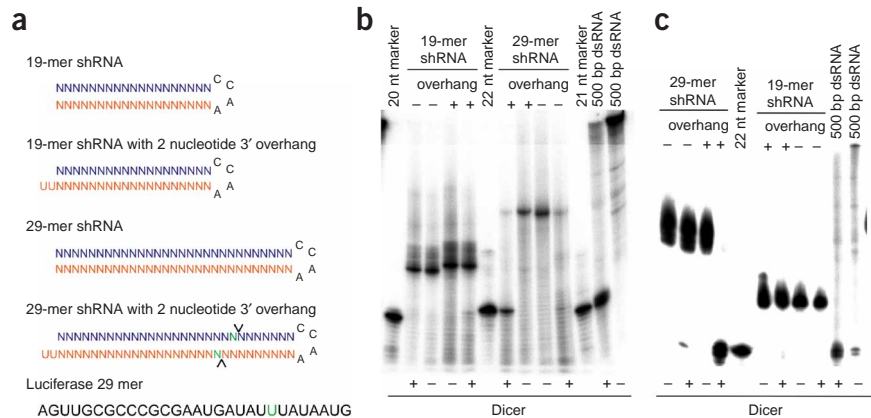
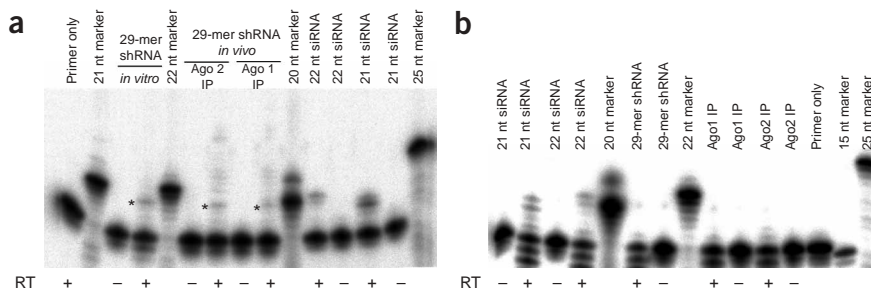


Figure 1 *In vitro* processing of 29-bp shRNAs by Dicer generates a predominant siRNA from the end of each short hairpin. (a) The set of shRNAs containing 19- or 29-bp stems and either with or without a 2-nt 3' overhang is depicted schematically. For reference, the 29-nt sequence from luciferase (top, blue) strand is given. The presumed cleavage sites (as predicted by analysis of Dicer processing products) are indicated in green and by the arrows. (b) *In vitro* Dicer processing of shRNAs. 5' end labeled substrates as depicted in a were incubated either in the presence or absence of recombinant human Dicer. Processing of a 500-bp blunt-ended dsRNA is shown for comparison. Markers are end labeled single-stranded synthetic RNA oligonucleotides. (c) Uniformly labeled shRNAs with structures as indicated in a were processed by Dicer to produce a small RNA product. Results of processing a 500-bp blunt-ended dsRNA are shown for comparison.

suggested identical cleavage specificities when shRNAs were exposed to Dicer either *in vitro* or in living cells (Fig. 2a). Control experiments using a luciferase 29-mer shRNA alone (without Myc-tagged Ago1 or Ago2 expression) or cells transfected with Myc-tagged Ago1 or Ago2 alone (no shRNA) did not yield extension products (Fig. 2b).

Although the inability of Dicer to effectively cleave shRNAs with 19-bp stems may seem at odds with the effective use of such structures for triggering RNAi using vector-based expression, there is presently no evidence that these RNAs require Dicer for their action. Indeed, our results using RNAi to deplete Dicer from cells suggest a strong dependence on Dicer for shRNAs with 29-bp stems, but little dependence for shRNAs with 19-bp stems (not shown). However, 19-mer shRNA do enter RISC. Human 293 cells that constitutively express Ago1 were transfected with siRNAs, 29-mer shRNAs or 19-mer shRNAs. RISC was recovered by immunoprecipitation and associated RNAs were examined by northern blotting. (Supplementary Fig. 2 online) The 29-mer shRNA with an overhang and the 22-mer siRNA both entered RISC, producing 22-nt small RNAs. The 19-mer shRNA

Figure 2 Primer extension analysis shows that similar small RNAs are generated by Dicer processing *in vitro* or *in vivo*. (a) Primer extension was used to analyze products from processing of overhang-containing 29-mer shRNAs *in vivo*. Total RNAs were extended with a specific primer that yields a 20-base product if cleavage occurs 22 bases from the 3' end of the overhang-containing RNA (see Fig. 1a). For comparison, extensions of *in vitro* processed material are also shown. Lanes labeled siRNA are extensions of synthetic RNAs corresponding to predicted siRNAs that would be released by cleavage 21 or 22 nt from the 3' end of the overhang-containing precursor. Observation of extension products depends entirely on the inclusion of reverse transcriptase (RT). The * indicates the specific extension product. Markers are phosphorylated, synthetic DNA oligonucleotides. (b) Total RNA from control transfections, which lacked a coexpressed tagged Ago protein, making it impossible to recover small RNAs in the immunoprecipitates, did not show a primer extension product. The same primer was used for all extensions and is compatible with all RNAs. Controls labeled Ago1 or Ago2 lacked co-transfected target RNAs.



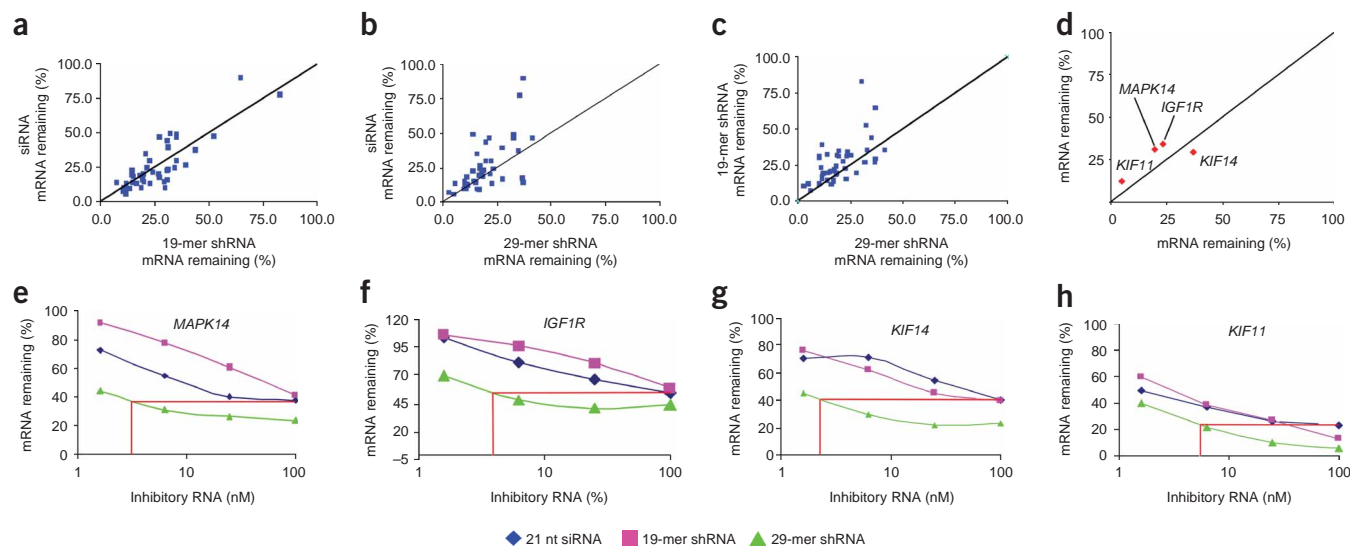


Figure 3 Gene suppression by shRNAs is comparable to or more effective than that achieved by siRNAs targeting the same sequences. (**a–c**) mRNA suppression by 43 siRNAs targeting six different genes was compared with suppression by 19-mer or 29-mer shRNAs derived from the same target sequences. 19-mer and 29-mer shRNAs were also directly compared. All RNAs were transfected at a final concentration of 100 nM. Values indicated on the x and y axes reflect the percentage of mRNA remaining after 24 h in HeLa cells transfected with RNA as compared with cells treated with transfection reagent alone. (**d–h**) Four representative sets of siRNA and 19-mer and 29-mer shRNAs were used in dose-response analysis to compare the potency of representative RNAi triggers targeting four genes. Comparisons of relative suppression (19-mer versus 29-mer) at the maximal dose are shown for reference in **d**. Titration curves were also performed reporting the percentage of target mRNA remaining (y axis) from transfections at 1.56, 6.25, 25 and 100 nM final concentrations of RNA (x axis). Percentage of RNA remaining was determined by semiquantitative RT-PCR. Gene targets were *MAPK14*, *KIF11*, *IGF1R* and *KIF14*. (Sequences used were MAPK14-4, KIF11-6, IGF1R-1, KIF14-1 as in **Supplementary Table 1**.) Blue diamonds, 21-mer siRNAs; pink squares, 19-mer shRNAs; green triangles, 29-mer shRNAs. Red lines indicate the concentration of 29-mer shRNA that gives the level of inhibition achieved by 100 nM siRNA.

also entered RISC but produced two distinct small RNAs of 21 and 23 nt. Although we do not understand the mechanistic basis for this observation, it may reflect Dicer-independent cleavage of the 19-mer shRNA in the loop by a single-strand specific ribonuclease.

Because we could predict which single, specific 22-nt sequence would be incorporated into RISC from a given shRNA, we could directly compare the silencing efficiency of shRNAs and siRNAs. Toward this goal, we selected 43 sequences targeting a total of 5 genes (3–9 sequences per gene). For each sequence, we synthesized a 21-mer siRNA (19-bp stem) and shRNAs with 19- or 29-bp stems that were predicted to give Dicer products that either were identical to their corresponding siRNAs or differed by the addition of one 3' nucleotide homologous to the target. Importantly, each was predicted to give precisely the same 5' end after cleavage of a 22-mer RNA from the shRNA (**Supplementary Fig. 3** online). Sequences for siRNAs are provided in **Supplementary Table 1** online. Each RNA species was transfected into HeLa cells at a relatively high concentration (100 nM). The level of suppression was determined by semiquantitative RT-PCR of RNA from HeLa cells 24 h after transfection and the performance of each shRNA was compared with the performance of the corresponding siRNA. Studies assessing siRNAs and 19-mer shRNAs showed that there was little difference in silencing at 24 h with these species (**Fig. 3a**). A comparison of siRNAs with shRNAs having 29-bp stems gave a different result. Clustering of the data points above the diagonal indicated consistently better inhibition with the 29-mer shRNAs (**Fig. 3b**). As predicted from the aforementioned results, direct comparisons of shRNAs with 19- and 29-bp stems indicated a greater overall effect with the latter structure (**Fig. 3c**).

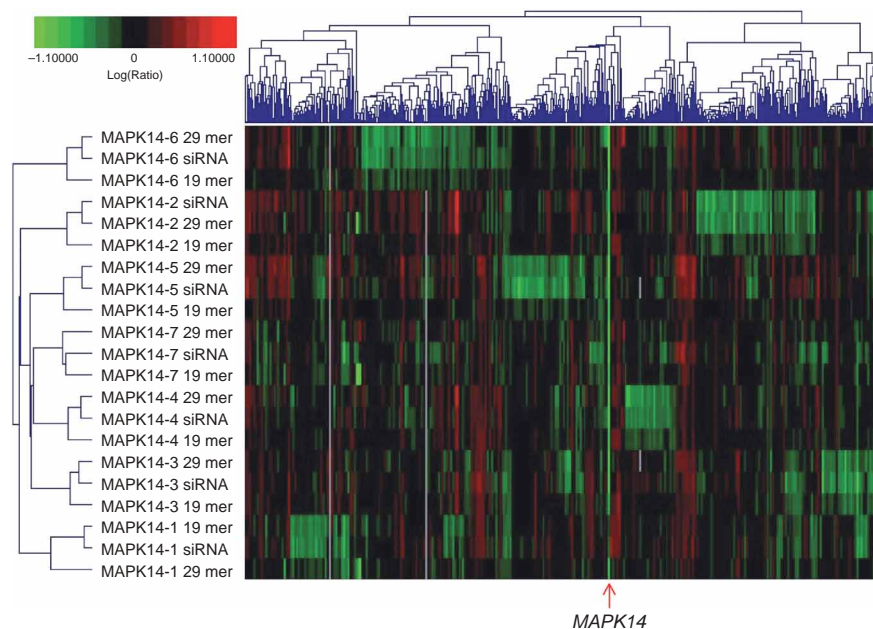
The generally better inhibition with 29-mer shRNAs at a high dose led us to investigate the potency of these silencing triggers as

compared with siRNAs. Seventeen complete sets comprising an siRNA, a 19-mer shRNA and a 29-mer shRNA were examined for suppression in titration experiments. In no case did the 19-mer shRNAs perform better than the corresponding siRNAs. In contrast, 29-mer shRNAs exceeded the performance of siRNAs in the majority of cases. In most cases, the 29-mer shRNAs showed greater inhibition at the maximal dose; however, even when this inhibition at the maximal dose did not differ much from the siRNA or 19-mer shRNA, the efficacy of the 29-mer at lower concentrations was substantially better. The dose-response experiments for four representative sets of RNAs are shown in **Figure 3d–h**.

Consistent with our results for most of the RNA sets tested, in the case of *MAPK14*, *KIF14* and *KIF11*, the maximal level of suppression for the 29-mer shRNA was approximately twofold greater than the maximal level of suppression for the corresponding siRNA (**Fig. 3e–h**). More importantly, in some cases, the amount of RNA required to achieve maximal inhibition was up to 20-fold lower with 29-mer shRNA than with a similar 21-mer siRNA. This greater potency for 29-mer shRNA as compared to the other two RNA species may reflect the entry of these RNAs into the RNAi pathway as natural intermediates and may explain their greater efficacy when delivered from vectors¹⁴.

Microarray analysis has shown downregulation of many nontargeted transcripts after transfection of siRNAs into HeLa cells²⁸. Notably, these gene expression signatures differed between different siRNAs targeting the same gene. Many of the 'off-target' transcripts contained sites of partial identity to the individual siRNA, possibly explaining the source of the effects. To examine potential off-target effects of synthetic shRNAs, we compared shRNA signatures with those of siRNAs derived from the same target sequence.

Figure 4 Microarray profiling shows that gene expression profiles of 29-mer shRNAs and the corresponding siRNAs are more similar than expression profiles of 19-mer shRNAs and the corresponding siRNAs. The 19-mer and 29-mer shRNAs and siRNAs designed for seven different target sequences within the coding region of *MAPK14* were tested for gene silencing 24 h after transfection into HeLa cells. Each row of the heat map reports the gene expression signature resulting from transfection of an individual RNA. Two-dimensional clustering of the data groups RNAs (vertical axis dendrogram) and regulated genes (horizontal axis dendrogram) according to signature similarities. Data shown represent genes that display at least a twofold change in expression level ($P < 0.01$ and \log_{10} intensity > 1) relative to mock-transfected cells. Green indicates decreased expression relative to mock transfection and red indicates elevated expression. Black indicates no change and gray indicates data with $P > 0.01$. The red arrow indicates *MAPK14*.



Using microarray gene expression profiling, we obtained a genome-wide view of transcript suppression. A two-dimensional clustering analysis of the signatures produced in HeLa cells 24 h after transfection of 19-mer and 29-mer shRNAs compared with those generated by corresponding siRNAs (Fig. 4) shows that each set of three RNAs derived from the same core sequence was accurately clustered. Furthermore, in all but two of seven cases, although the 19-mer shRNAs produced signatures similar to those of the corresponding siRNAs, the signatures of the 29-mer shRNAs were more closely related to those of the corresponding siRNAs. In one of the two cases in which the 19-mer shRNA and the siRNA clustered more closely (*MAPK14-1*), these two RNA species did not appreciably silence the target gene, whereas the 29-mer shRNA did. The agreement between the signatures of 29-mer shRNAs and siRNAs is consistent with precise processing of the shRNA to generate a single siRNA rather than a random sampling of the hairpin stem by Dicer. The overall smaller signature sizes of the 19-mer shRNA and the basis of their divergence from the signature of the corresponding siRNA are presently unclear. However, extensive analysis of off-target effects potentially associated with these shRNAs was not our goal.

Considered together, our results suggest that chemically synthesized 29-mer shRNAs can be substantially more effective triggers of RNAi than can siRNAs. A mechanistic explanation for this finding may lie in the fact that 29-mer shRNAs are substrates for Dicer processing both *in vitro* and *in vivo*. We originally suggested that siRNAs might be passed from Dicer to RISC in a solid-state reaction on the basis of an interaction between Dicer and Argonaute 2 in *D. melanogaster* S2 cell extracts⁴. More recently, results from several laboratories have strongly suggested a model for assembly of the RNAi effector complex in which a multiprotein assembly containing Dicer and accessory proteins interacts with an Argonaute protein and actively loads one strand of the siRNA or miRNA into RISC^{18–20}. Such a model implies that Dicer substrates, derived from nuclear processing of pri-miRNAs or cytoplasmic delivery of pre-miRNA mimetics, might be loaded into RISC more effectively than siRNAs. Our data support such a prediction, as it is not the hairpin structure of the synthetic RNA that determines its increased efficacy, but the fact that the shRNA is a Dicer substrate that

correlates with enhanced potency, as is reported in an accompanying paper in this issue²⁹. In *D. melanogaster*, Dicer is also required for siRNAs to enter RISC, and similar data have been obtained in mammalian cells^{18,30}. Thus, it is possible that even siRNAs enter RISC via a Dicer-mediated assembly pathway and that our data simply reflect an increased affinity of Dicer for longer duplex substrates. Alternatively, hairpin RNAs, such as miRNA precursors, might interact with specific cellular proteins that facilitate delivery of these substrates to Dicer, whereas siRNAs might not benefit from such chaperones. Overall, our results suggest an improved method for triggering RNAi in mammalian cells using higher potency RNAi triggers. This remains a critical issue both for cell culture studies and for potential therapeutic use *in vivo*. Mapping the predominant 22-nt sequence that appears in RISC from each of these shRNAs now permits the combination of this more effective triggering method with rules for effective siRNA design.

METHODS

RNA sequence design. Each set of RNAs began with the choice of a single 19-mer sequence. These 19-mers were used directly to create siRNAs. To create shRNAs with 19-mer stems, we appended a four-base loop (either CCAA or UUGG) to the end of the 19-mer sense strand target sequence followed by the 19-mer complementary sequence and a UU overhang. We tested a variety of loop sequences and noted no significant influence of the sequences on the performance of triggers. To create 29-mer stems, we increased the length of the 19-mer target sequence by adding one base upstream and nine bases downstream from the target region and used the same loop sequence and UU overhang. All synthetic RNA molecules used in this study were purchased from Dharmacon.

Dicer processing. RNA hairpins corresponding to luciferase were end-labeled with [γ -³²P]ATP and T4 polynucleotide kinase (PNK), and 0.1 pmol of RNA was processed with 2 units of Dicer (Stratagene) at 37 °C for 2 h. Reaction products were Trizol extracted, isopropanol precipitated and separated on an 18% polyacrylamide, 8 M urea denaturing gel. For RNase III digestion, 0.1 pmol was digested with 1 unit of *E. coli* RNase III (NEB) for 30 min at 37 °C and analyzed as described above. Uniformly labeled hairpins were produced using a T7 Megashortscript kit (Ambion) with [α -³²P]UTP and then incubated with Dicer as indicated above.

For primer extension analysis, hairpins were processed with Dicer at 37 °C for 2 h; this was followed by heat inactivation of the enzyme. The sequence of the primer is the first 16 nt from the 5' end of the hairpin: 5'-AGTTGCGCCCGCAAC-3'. DNA primers were 5' labeled with PNK and annealed to 0.05 pmol of RNA as follows: 95 °C for 1 min, 10 min at 50 °C and then 1 min on ice. Extensions were carried out at 42 °C for 1 h using MoMLV reverse transcriptase. Products were analyzed by electrophoresis on a 8 M urea/20% polyacrylamide gel.

For analysis of *in vivo* processing, Linx cells were transfected in 10-cm plates using Mirus TKO (10 µg hairpin RNA) or Mirus LT4 reagent for DNA transfection (12 µg of AGO1 or AGO2 DNA)⁶. 293 cells constitutively expressing Ago1 were used for northern blot experiments. Cells were lysed and immunoprecipitated after 48 h using antibody to Myc (9E14). Immunoprecipitates were washed three times in lysis buffer and treated with DNase I for 15 min. Immunoprecipitates were then primer extended as described above.

siRNA and shRNA transfections and mRNA quantification. HeLa cells were transfected in 96-well plates using Oligofectamine (Invitrogen) with the final nanomolar concentrations of each synthetic RNA indicated in the graphs. RNA quantitation was performed by real-time PCR, using appropriate Applied Biosystems TaqMan primer probe sets 24 h after RNA transfection, and the percentage of mRNA remaining was compared with cells treated with transfection reagent alone.

Microarray gene expression profiling. HeLa cells were transfected in six-well plates with 100 nM final concentration of the appropriate RNA using Oligofectamine (according to the manufacturer's instructions). RNA from transfected cells was hybridized competitively with RNA from mock-transfected cells (those treated with transfection reagent in the absence of synthetic RNA). Total RNA was purified by the Qiagen RNeasy kit, and processed as described previously²⁸ for hybridization to microarrays containing oligonucleotides corresponding to approximately 21,000 human genes. Ratio hybridizations were performed with fluorescent label reversal to eliminate dye bias. Microarrays were purchased from Agilent Technologies. Error models have been described previously²⁸. Data were analyzed using Rosetta Resolver software.

Note: Supplementary information is available on the Nature Biotechnology website.

ACKNOWLEDGMENTS

G.J.H. is supported by an Innovator Award from the U.S. Army Breast Cancer Research Program. This work was also supported by a grant from the US National Institutes of Health (G.J.H.). D.S. is supported by a predoctoral fellowship from the US Army Breast Cancer Research Program. We thank the Rosetta Gene Expression Laboratory for microarray RNA processing and hybridizations.

COMPETING INTERESTS STATEMENT

The authors declare competing financial interests (see the *Nature Biotechnology* website for details).

Received 30 July; accepted 2 November 2004

Published online at <http://www.nature.com/naturebiotechnology/>

- Zamore, P.D., Tuschl, T., Sharp, P.A. & Bartel, D.P. RNAi: double-stranded RNA directs the ATP-dependent cleavage of mRNA at 21 to 23 nucleotide intervals. *Cell* **101**, 25–33 (2000).

- Hammond, S.M., Bernstein, E., Beach, D. & Hannon, G.J. An RNA-directed nuclease mediates post-transcriptional gene silencing in *Drosophila* cells. *Nature* **404**, 293–296 (2000).
- Bernstein, E., Caudy, A.A., Hammond, S.M. & Hannon, G.J. Role for a bidentate ribonuclease in the initiation step of RNA interference. *Nature* **409**, 363–366 (2001).
- Hammond, S.M., Boettcher, S., Caudy, A.A., Kobayashi, R. & Hannon, G.J. Argonaute2, a link between genetic and biochemical analyses of RNAi. *Science* **293**, 1146–1150 (2001).
- Song, J.J., Smith, S.K., Hannon, G.J. & Joshua-Tor, L. Crystal structure of Argonaute and its implications for RISC slicer activity. *Science* **305**, 1434–1437 (2004).
- Liu, J. *et al.* Argonaute2 is the catalytic engine of mammalian RNAi. *Science* **305**, 1437–1441 (2004).
- Elbashir, S.M. *et al.* Duplexes of 21-nucleotide RNAs mediate RNA interference in cultured mammalian cells. *Nature* **411**, 494–498 (2001).
- Bartel, D.P. MicroRNAs: genomics, biogenesis, mechanism, and function. *Cell* **116**, 281–297 (2004).
- Lee, Y. *et al.* The nuclear RNase III Drosha initiates microRNA processing. *Nature* **425**, 415–419 (2003).
- Hutvagner, G. *et al.* A cellular function for the RNA-interference enzyme Dicer in the maturation of the let-7 small temporal RNA. *Science* **293**, 834–838 (2001).
- Ketting, R.F. *et al.* Dicer functions in RNA interference and in synthesis of small RNA involved in developmental timing in *C. elegans*. *Genes Dev.* **15**, 2654–2659 (2001).
- Grishok, A. *et al.* Genes and mechanisms related to RNA interference regulate expression of the small temporal RNAs that control *C. elegans* developmental timing. *Cell* **106**, 23–34 (2001).
- Brummelkamp, T.R., Bernards, R. & Agami, R. A system for stable expression of short interfering RNAs in mammalian cells. *Science* **296**, 550–553 (2002).
- Paddison, P.J., Caudy, A.A., Bernstein, E., Hannon, G.J. & Conklin, D.S. Short hairpin RNAs (shRNAs) induce sequence-specific silencing in mammalian cells. *Genes Dev.* **16**, 948–958 (2002).
- Zeng, Y., Wagner, E.J. & Cullen, B.R. Both natural and designed micro RNAs can inhibit the expression of cognate mRNAs when expressed in human cells. *Mol. Cell* **9**, 1327–1333 (2002).
- Schwarz, D.S. *et al.* Asymmetry in the assembly of the RNAi enzyme complex. *Cell* **115**, 199–208 (2003).
- Khorova, A., Reynolds, A. & Jayasena, S.D. Functional siRNAs and miRNAs exhibit strand bias. *Cell* **115**, 209–216 (2003).
- Lee, Y.S. *et al.* Distinct roles for *Drosophila* Dicer-1 and Dicer-2 in the siRNA/miRNA silencing pathways. *Cell* **117**, 69–81 (2004).
- Pham, J.W., Pellino, J.L., Lee, Y.S., Carthew, R.W. & Sontheimer, E.J. A Dicer-2-dependent 80s complex cleaves targeted mRNAs during RNAi in *Drosophila*. *Cell* **117**, 83–94 (2004).
- Tomari, Y. *et al.* RISC assembly defects in the *Drosophila* RNAi mutant armitage. *Cell* **116**, 831–841 (2004).
- Zhang, H., Kolb, F.A., Brondani, V., Billy, E. & Filipowicz, W. Human Dicer preferentially cleaves dsRNAs at their termini without a requirement for ATP. *EMBO J.* **21**, 5875–5885 (2002).
- Lund, E., Guttinger, S., Calado, A., Dahlberg, J.E. & Kutay, U. Nuclear export of microRNA precursors. *Science* **303**, 95–98 (2004).
- Ma, J.B., Ye, K. & Patel, D.J. Structural basis for overhang-specific small interfering RNA recognition by the PAZ domain. *Nature* **429**, 318–322 (2004).
- Lingel, A., Simon, B., Izaurralde, E. & Sattler, M. Structure and nucleic-acid binding of the *Drosophila* Argonaute 2 PAZ domain. *Nature* **426**, 465–469 (2003).
- Song, J.J. *et al.* The crystal structure of the Argonaute2 PAZ domain reveals an RNA binding motif in RNAi effector complexes. *Nat. Struct. Biol.* **10**, 1026–1032 (2003).
- Yan, K.S. *et al.* Structure and conserved RNA binding of the PAZ domain. *Nature* **426**, 468–474 (2003).
- Zhang, H., Kolb, F.A., Jaskiewicz, L., Westhof, E. & Filipowicz, W. Single processing center models for human Dicer and bacterial RNase III. *Cell* **118**, 57–68 (2004).
- Jackson, A.L. *et al.* Expression profiling reveals off-target gene regulation by RNAi. *Nat. Biotechnol.* **21**, 635–637 (2003).
- Rossi, J.J. *et al.* Synthetic dsRNA Dicer substrates enhance RNAi potency and efficacy. *Nat. Biotechnol.* **23**, in the press (2005).
- Doi, N. *et al.* Short-interfering-RNA-mediated gene silencing in mammalian cells requires Dicer and eIF2C translation initiation factors. *Curr. Biol.* **13**, 41–46 (2003).